Local-environment effects on the density of states and substitutional impurities in random alloys

Javier E. Hasbun and Laura M. Roth
Department of Physics, State University of New York at Albany, 1400 Washington Avenue, Albany, New York 12222
(Received 14 July 1987)

We study the electronic structure of a binary alloy using the effective-medium approximation (EMA) and we include the local environment by treating the system as a multicomponent alloy with different neighbor compositions. We use a tight-binding model in the nearest-neighbor approximation. On introducing an impurity a spectrum of levels is found. A simplified EMA which includes the local environment is developed which is as easy to evaluate as the coherent-potential approximation. By making a perturbation about the virtual-crystal approximation a simple scheme which models the splitting of impurity levels is found. We extend the EMA to consider the effects of short-range order with nonrandom correlations and find that our approximations reduce to the exact results in the appropriate limits.

I. INTRODUCTION

One of the standard methods for trying to understand the physical properties of random systems is the Green's-function formalism. The coherent-potential approximation (CPA) of Soven,[1] and Velicky, Kirkpatrick, and Ehrenreich[2] for the case of electronic states in random alloys, and of Taylor[3] for the case of vibrational properties, has stood out as the most effective single-site approximation. The CPA as originally proposed and applied for example to a single tight-binding band in a two-component alloy system with diagonal disorder is useful at all values of the concentration and scattering strength. A number of other applications are reviewed by Elliot, Krumhansl, and Leath.[4] Another feature of the single-site CPA is that the Green's function is analytic and has a negative imaginary part, leading to positive density of states.[5–7] However, the CPA has other nonphysical features such as a k-independent self-energy and an impurity band with no structure.[8,9]

During the last decade there have been extensions of the CPA involving off-diagonal disorder,[10–14,15] larger cluster (pair, triplet, etc.) scattering,[6,16–21] short-range order, and local environment.[20,15,22–25] An excellent review of extensions beyond the CPA has been given by Leath[26] (see also, Elliot *et al.*[4]). The general problem of including off-diagonal disorder in addition to diagonal disorder was solved most completely by Blackman, Esterling, and Berk.[12] These authors introduced a conditionally averaged site-site Green's function using a locator approach, and replaced the hopping matrix elements by 2×2 matrices. It became clear from this work that any locator theory which works for diagonal disorder can be readily generalized to include off-diagonal disorder by their method.

Early attempts to go beyond the single-site CPA to include clusters larger than one led to nonanalyticities in the Green's function.[27] Cluster theories which have been shown to be analytic are the molecular CPA (MCPA) of Tsukada,[16] and the traveling cluster approximation (TCA) of Mills and Ratanavararaksa.[6] In general, the molecular CPA has the drawback of not having the full translational symmetry of the lattice. However, for the case of pseudobinary semiconductor alloys Hass *et al.*[28] were able to use a translationally invariant MCPA in their study. The TCA does maintain translational invariance, though it is computationally rather complicated. The augmented space formalism of Mookerjee,[18] as discussed by Diehl and Leath,[29] has been used by Kaplan *et al.*[15] to extend the TCA to include off-diagonal disorder, environmental disorder, and short-range order. Extensions to model cluster effects in liquids by Sen *et al.*[21] have been disappointing. The augmented space formalism has also been used by Mookerjee and co-workers[19] together with the recursion method of Haydock and co-workers[30] to generate analytic cluster CPA's (see Ref. 19).

We are particularly interested here in studying environmental effects for alloy systems, and especially systems with impurities. For example, impurities in semiconductor alloys experience different local environments due to the random composition of the host alloy.[31] Much of the work in this area has been based on the embedded-cluster method of Gonis and Garland,[24] which has been studied by Myles and Dow for phonon spectra and electronic structure[32] in one-dimensional binary alloys including environmental effects on impurity levels. This method has been extended to ternary alloys, short-range order,[32] and local environment effects on impurities in realistic models of semiconductor alloys.[33] The embedded-cluster method in which a cluster is embedded in a CPA or VCA medium is analytic but not translationally invariant[26] and does not have a self-consistently determined medium. The advantage is that details of configurations of the embedded cluster can be studied. There have also been semiempirical calculations based on a kind of local VCA.[34]

The search for a simple single-site theory which can

be extended to include off-diagonal disorder, short-range order, and local environment, and which can be extended to the study of the local environment effects on impurity levels, has led us to consider the effective-medium approximation (EMA) of Roth.[35] The EMA was originally proposed for liquid metals,[35] and later extended to liquid alloys.[36] It is a natural extension of the CPA to include short-range order while remaining a single-site theory with translational invariance. The EMA was further extended to studies of magnetic excitations in antiferromagnetic alloys where local environment effects are important.[37] This last work was based on a multicomponent EMA in which different local environments are regarded as different components of an effective alloy. In this work we will use the multicomponent EMA to study local environment effects in alloys, taking advantage of its single-site property and translational invariance. We will refer to the multicomponent EMA as simply the EMA. In this work we will also investigate the analytic properties of the theory where possible. We will work with the tight-binding model with nearest-neighbor interactions. The theory can handle off-diagonal disorder, and has been extended to realistic systems such as semiconductors.[38] In Sec. II we discuss the model, and in Secs. III and IV we present our work for the simplest case, the split-band limit. In Sec. V we include the impurity for the split-band-limit case. Sections VI, VII, and VIII deal with the more complicated case of the two-component alloy, and in Sec. IX we generalize the impurity result to the two-component alloy. In Sec. X we discuss a perturbational approach to impurity level splitting due to environment. In Secs. XI and XII we include short-range order due to nonrandom correlations. In Sec. XIII we discuss the results followed by our conclusion in Sec. XIV.

II. THE MODEL

We consider a one-orbital tight-binding-model Hamiltonian in the Wannier representation

$$H_0=\sum_n |n\rangle\varepsilon_n\langle n| + \sum_{\substack{n,m\\ n\neq m}} |n\rangle V_{nm}\langle m| \ . \tag{2.1}$$

The diagonal energies ε_n can take on the values ε_A or ε_B depending on the type of atom occupying site n. The off-diagonal hopping integrals V_{nm} between sites n and m, in general, depend on the type of atoms A or B occupying sites n and m. To model the local environment we assume that the major factor will be the composition of the nearest-neighbor shell, and so we introduce an index s which measures the number of B nearest neighbors, and treat the system as a multicomponent alloy of different local environments. We define ${}^r\rho_i^s$ to be an occupation index which takes on the value of zero, unless i is an r site (A or B) with s B neighbors, in which case it is one. Let ${}^rx^s$ be the concentration of r sites with s B neighbors, readily obtained from the binomial distribution function, and let ${}^{rr'}g_{ij}^{ss'}$ be the pair distribution function such that $({}^{rr'}g_{ij}^{ss'})({}^{r'}x^{s'})$ is equal to the probability that there will be an r' component with s' B neighbors on site j, given that there is an r component with s B neighbors on site i. The concentration of B and A sites with s B neighbors is given for the random alloy by

$${}^Bx^s=\begin{bmatrix} z \\ s \end{bmatrix} c^s(1-c)^{z-s}c \ , \tag{2.2a}$$

$${}^Ax^s=\begin{bmatrix} z \\ s \end{bmatrix} c^s(1-c)^{z-s}(1-c) \ , \tag{2.2b}$$

where c is the concentration of occupied B sites and z the number of nearest neighbors.

Considering nearest neighbors, the pair distribution functions according to our definition above, are given for the random alloy by

$$\begin{aligned} {}^{BB}g^{ss'}&=\frac{s}{cz}\left[\frac{x_B^{s'-1}(z-1)}{x_B^{s'}(z)}\right]=\beta_s\beta_{s'}, \quad {}^{BA}g^{ss'}=\alpha_s\beta_{s'} \\ {}^{AB}g^{ss'}&=\beta_s\alpha_{s'}, \quad {}^{AA}g^{ss'}=\alpha_s\alpha_{s'} \end{aligned} \tag{2.3}$$

where

$$\alpha_s=\frac{z-s}{(1-c)z}, \quad \beta_s=\frac{s}{cz} \ . \tag{2.4}$$

These expressions are exact for bcc, simple cubic (sc), and zinc-blende structures without short-range order, but they are only approximate for interlocking systems like fcc, where they neglect sharing of neighbors.[24] One can calculate ${}^{rr'}g_{ij}^{ss'}$ for such systems as well as for further than nearest neighbors, but we will not require them here. We also have the following identities:

$$\frac{1}{c^r}\sum_s x_r^s=1, \quad \sum_{s',r'} {}^{rr'}g^{ss'}x_{r'}^{s'}=1 \ , \tag{2.5}$$

where ${}^{rr'}g^{ss'}={}^{r'r}g^{s's}$ is symmetric, and c^r is the concentration of species r.

From the matrix representation of the work of Blackman *et al.*,[12] the total Green's function equals the sum of the averaged site-site Green's functions. We generalize this result to include the environment by writing

$$G_{ij}=\langle \mathcal{G}_{ij}\rangle=\sum_{\substack{r,r'\\ s,s'}}\langle {}^{rr'}\mathcal{G}_{ij}^{ss'}\rangle=\sum_{\substack{r,r'\\ s,s'}} {}^{rr'}G_{ij}^{ss'} \ , \tag{2.6}$$

where the exact Green's function $\mathcal{G}$ is given by

$${}^{rr'}\mathcal{G}_{ij}^{ss'}={}^r\rho_i^s L_i\left[\delta_{ij}\delta_{rr'}\delta_{ss'}+\sum_{l,r''s''} {}^{rr''}V_{il}^{ss''}\,{}^{r''r}\mathcal{G}_{lj}^{s''s'}\right] \tag{2.7}$$

and where the locator $L_i=(\omega-\varepsilon_i)^{-1}$. Equation (2.7), in general, includes off-diagonal disorder and short-range order. In this paper we specialize to diagonal disorder only for the simple-cubic system.

III. APPROXIMATIONS, SPLIT-BAND LIMIT ($\varepsilon_A\to\infty$, $\varepsilon_B\equiv 0$)

A. EMA

In the effective-medium approximation (EMA) the actual system is replaced by an effective medium whose properties are self-consistently determined by requiring that on the average, the result of examining the scattering by a particular site of the system, by first removing it

and then putting it back, be equal to the original effective medium. This procedure is the same one used to derive the original CPA.[2] The result of including short-range order correlations in the CPA, however, is to introduce the pair distribution function of Sec. II and to obtain the EMA equations[35,37] which we write for the split-band limit and in the momentum representation as

$$G_k^{ss'}=x^s L^s\left[\delta_{ss'}+\sum_{s''} M_k^{ss''}G_k^{s''s'}\right], \tag{3.1}$$

$$L^s=(\omega-\Sigma_d^s)^{-1}, \tag{3.2}$$

$$\Sigma_d^s=\frac{1}{N}\sum_{k,s',s''} V_k G_k^{s's''}M_k^{s''s}, \tag{3.3}$$

$$M_k^{ss'}=V_k g^{ss'}+\Sigma_{1k}^{ss'}, \tag{3.4}$$

$$\Sigma_{1k}^{ss'}=\frac{1}{N}\sum_{k',s'',s'''} \mathcal{A}^{ss'}(k-k')M_{k'}^{ss''}G_{k'}^{s''s'''}M_{k'}^{s'''s'}, \tag{3.5}$$

where for the split-band-limit case $\varepsilon_A\to\infty$ the only pair distribution function needed is ${}^{BB}g^{ss'}$, and so we do not need to use the species index. Equation (3.1) is the EMA Green's function which involves the effective locator, Eq. (3.2), and the effective interactor, Eq. (3.4). We note that the locator involves the diagonal self-energy of Eq. (3.3), while the interactor involves the k-dependent off-diagonal self-energy of Eq. (3.5).

The quantity $\mathcal{A}^{ss'}(k-k')$ in Eq. (3.5) is given by

$$\mathcal{A}^{ss'}(k-k')=\sum_i \{\exp[i(k-k')R_{i0}]\}(g_{i0}^{ss'}-1), \tag{3.6}$$

where

$$g_{ij}^{ss'}=\begin{cases}0 & \text{for } i=j\\ g^{ss'}=\beta_s\beta_{s'} & \text{for nearest neighbors}\\ \bar{g}^{ss'} & \text{beyond nearest neighbors},\end{cases} \tag{3.7}$$

where β_s is given in Eq. (2.4). We next make the approximation of neglecting the k dependence in Eq. (3.5), i.e., we take $h^{ss'}(k-k')=-1$, to get for the off-diagonal self-energy

$$\Sigma_{1k}^{ss'}\to\Sigma_1^{ss'}=-\frac{1}{N}\sum_{k,s'',s'''} M_k^{ss''}G_k^{s''s'''}M_k^{s'''s'}. \tag{3.8}$$

Thus we will not need $\bar{g}_{ij}^{ss'}$ beyond nearest neighbors, since it enters only through Eq. (3.4).

We solve the above equations by first making the ansatz

$$M_k^{ss'}=g^{ss'}M_k, \tag{3.9}$$

where from above $g^{ss'}=\beta_s\beta_{s'}$ is separable with $\beta_s=s/cz$. With these assumptions, we find the solution for $G_k^{ss'}$ to be

$$G_k^{ss'}=x^sL^s[\delta_{ss'}+\beta_s x^{s'}L^{s'}\beta_{s'}M_k(1-F_2M_k)^{-1}], \tag{3.10}$$

where

$$F_n=\sum_s x^sL^s\beta_s^n. \tag{3.11}$$

Using Eq. (2.6), we find for the total Green's function G_k,

$$G_k=F_0+F_1^2M_k(1-F_2M_k)^{-1}. \tag{3.12}$$

We can find M_k by substituting Eqs. (3.9) and (3.10) into Eq. (3.8), and with the use of Eq. (3.4) we obtain

$$M_k=V_k+\sigma,\quad \Sigma_1^{ss'}=g^{ss'}\sigma, \tag{3.13}$$

$$\sigma=-\frac{1}{N}\sum_k\frac{F_2M_k^2}{1-F_2M_k}. \tag{3.14}$$

By making use of the fact that $(1/N)\sum_k V_k=0$, we can write the left-hand side of Eq. (3.14) as $(1/N)\sum_k M_k$, to obtain the important identity

$$\sum_k\frac{M_k}{1-F_2M_k}=0, \tag{3.15}$$

which expresses the site exclusion property. Also, from Eq. (3.3) we have

$$\Sigma_d^s=\beta_s\sigma_d,\quad \frac{1}{N}\sum_k\frac{F_1V_kM_k}{1-F_2M_k}=\sigma_d=-\left[\frac{F_1}{F_2}\right]\sigma, \tag{3.16}$$

the last identity coming from Eqs. (3.14) and (3.15). Equation (3.15) allows us to obtain the density of states from Eq. (3.12),

$$n(\omega)=-\frac{1}{\pi}\mathrm{Im}\frac{1}{N}\sum_k G_k=-\frac{1}{\pi}\mathrm{Im}(F_0). \tag{3.17}$$

B. CPA

The CPA is obtained from the EMA for the split-band limit by neglecting correlation, i.e., letting $g^{ss'}\to 1$. Then from Eq. (3.12) with $F_n\to\tilde{L}\equiv cL$ we have

$$G_k=\frac{\tilde{L}}{1-\tilde{L}M_k}=\frac{c}{\omega-cV_k-(1-c)\Sigma_d}, \tag{3.18}$$

where we have used $M_k=V_k-\Sigma_d$, $L=(\omega-\Sigma_d)^{-1}$, and where Σ_d is obtained self-consistently from

$$\Sigma_d=\frac{1}{N}\sum_k M_k^2G_k=\frac{1}{N}\sum_k V_kM_kG_k. \tag{3.19}$$

The usual form of the CPA (Ref. 2) is obtained by substituting

$$(\tilde{L}^{-1}+\Sigma_d)=\frac{1}{c}[\omega-(1-c)\Sigma_d]=\omega-\Sigma$$

in Eq. (3.18). The coherent potential Σ in the CPA is the effective medium $\omega-(\tilde{L}^{-1}+\Sigma_d)$ in the EMA. The density of states is obtained from Eq. (3.18) by using Eqs. (3.12) and (3.15), giving

$$n(\omega)=-\frac{1}{\pi}\mathrm{Im}\frac{1}{N}\sum_k G_k=-\frac{1}{\pi}\mathrm{Im}(\tilde{L}). \tag{3.20}$$

IV. MOMENTS AND ANALYTIC PROPERTIES, SPLIT-BAND LIMIT

The moments in the locator approach are obtained as in Ref. 2. For the exact moments we expand

TABLE I. Comparison of the EMA and the SEMA moments of Secs. IV and VIII, respectively, in the split-band limit with the exact moments for this limit of the random-alloy case. Also, the moments for the correlated CPA of Sec. XII in the split-band limit are compared with the exact moments in the nonrandom case for this limit.

	Moments			
	M_0	M_1	M_2	M_3
			Random case	
Exact	c	c^2V_k	$c^2(1-c)I_2+c^3V_k^2$	$c^3(1-c)I_3+2c^3(1-c)I_2V_k+c^4V_k^3$
SEMA	c	c^2V_k	$c^2(1-c)I_2+c^3V_k^2$	$c^3(1-c)I_3+2cV_kI_2\left[\frac{1+c(z-1)}{cz}-c^2\right]+c^4V_k^3$
EMA	c	c^2V_k	$c^2\left[1-\frac{1+c(z-1)}{z}\right]I_2+c^2\left[\frac{1+c(z-1)}{z}\right]V_k^2$	
			Correlated case	
Exact	c	c^2gV_k	$c^2g(1-cg)I_2+c^3g^2V_k^2$	
CPA	c	c^2gV_k	$c^2(1-c)g^2I_2+c^3g^2V_k^2$	

$$I_n\equiv\frac{1}{N}\sum_k V_k^n,\quad g\equiv {}^{BB}g=\frac{P_{BB}}{c}$$

$$G_k=\left\langle\frac{1}{N}\sum_{i,j}\mathcal{G}_{ij}\exp[ik(R_i-R_j)]\right\rangle$$

in powers of ω^{-1}. The nth moment $M^n(k)$ is the coefficient of $\omega^{-(n+1)}$ term in the expansion of G_k. The nth moment of the density of states is obtained from $M^n(k)$ by averaging over k. For the EMA the zeroth and first moments are given correctly and the second deviates from the exact result as shown in Table I. The error in the second moment is of the order of $1/z$, and it appears to be due to the approximation of $\Delta(k-k')=-1$ in Eq. (3.8), and in particular the neglect of the second and third neighbor part of Δ. For the moments of the density of states the EMA conserves the zeroth, first, and second while the third moment, in general, deviates from the exact result, but for the simple-cubic case, because of symmetry, it is conserved. The CPA conserves moments of the density of states at least through the fifth.[2]

The analytic properties of the above EMA can be studied from Eq. (3.15), from which we obtain the relation

$$F_2=\frac{1}{N}\sum_k\frac{1}{F_2^{-1}-cF_1^{-1}+\omega-V_k}\ , \tag{4.1}$$

where

$$F_n=\sum_s x^sL^s\beta_s^n,\quad \beta_s=\frac{s}{cz},\quad L^s=(\omega-\beta_s\sigma_d)^{-1}\ , \tag{4.2}$$

and where we have used the identity[37] $\omega F_1-\sigma_dF_2=c$. We note that Eq. (4.1) is also a self-consistent equation for σ_d. In order to have a positive density of states in Eq. (3.17) the functions F_n and also σ_d must have negative imaginary parts. From Eq. (4.1) this is possible if in the right-hand side we have

$$\mathrm{Im}(F_2^{-1})\geq\mathrm{Im}(cF_1^{-1})\ . \tag{4.3}$$

We can choose the sign of σ_d'' in the first guess of σ_d in Eq. (4.2), and we expect that the F_n's should be very close, and since $c\leq 1$ it is plausible that Eq. (4.3) should hold. More precisely, we find that a sufficient condition for the inequality of Eq. (4.3) to be satisfied in subsequent iterations of Eq. (4.1) is that $\omega c>\sigma_d'$, where σ_d' and σ_d'' are the real and imaginary parts of σ_d, respectively. For the case of the simple-cubic model our results do not violate this condition.[38]

V. IMPURITY IN ALLOY, SPLIT-BAND LIMIT

We note that from the previous result of Sec. III the diagonal part of the host Green's function is obtained from Eq. (3.17) for the EMA but from Eq. (3.20) for the CPA. These diagonal Green's functions involve the locators

$$L^s=(\omega-\varepsilon_B-\Sigma_d^s)^{-1} \tag{5.1}$$

for the EMA, and

$$L=(\omega-\varepsilon_B-\Sigma_d)^{-1} \tag{5.2}$$

for the CPA, where we have put back ε_B for clarity. We note that in the locator theories[12] the diagonal self-energies Σ_d^s and Σ_d for the EMA and the CPA, respectively, refer to the rest of the system not including the site at the origin ε_B. These self-energies are determined from Sec. III. We therefore replace the diagonal energy ε_B by the impurity diagonal energy ε_C in the locators of Eqs. (5.1) and (5.2) in a similar way as the Koster-Slater model.[39] For the CPA the local density of states[40] at the impurity site is

$$n(\omega)=-\frac{1}{\pi}\mathrm{Im}\left[\frac{1}{\omega-\varepsilon_c-\Sigma_d}\right]\ , \tag{5.3}$$

while for the EMA we weight the locator L^s by the distribution of local environments

$$n(\omega)=-\frac{1}{\pi}\mathrm{Im}\left[\sum_s \frac{x^s}{\omega-\varepsilon_c-\Sigma_d^s}\right],$$
$$x^s=\begin{bmatrix} z \\ s \end{bmatrix} c^s(1-c)^{z-s}. \tag{5.4}$$

The basic difference between the CPA Eq. (5.3) and the EMA Eq. (5.4) results is that we have a pole characteristic of each neighbor configuration s in the impurity local density of states for the EMA, but only one pole characteristic of the average configuration in the CPA. The energy at which these poles occur correspond to the impurity energy levels.[32,33,38]

VI. THE TWO-COMPONENT ALLOY

A. EMA

The EMA equations for the two-component alloy are similar to those used in the split-band limit of Sec. III, but we now include all indices, species, and environment:

$${}^{rr'}G_k^{ss'}={}^{r}x^{s}\,{}^{r}L^{s}\left[\delta_{ss'}\delta_{rr'}+\sum_{s'',r''}({}^{rr''}M_k^{ss''})({}^{r''r'}G_k^{s''s'})\right], \tag{6.1}$$

$${}^{rr'}M_k^{ss'}={}^{rr'}g^{ss'}V_k+{}^{rr'}\Sigma_1^{ss'}, \tag{6.2}$$

$${}^{rr'}\Sigma_1^{ss'}\,{}^{r'}x^{s'}\,{}^{r'}L^{s'}=-\frac{1}{N}\sum_k V_k\sum_{r'',s''}({}^{rr''}g^{ss''})({}^{r''r'}G_k^{s''s'}), \tag{6.3}$$

$${}^{r}\Sigma_d^{s}=-\sum_{r',s'}{}^{rr'}\Sigma_1^{ss'}\,{}^{r'}x^{s'}, \tag{6.4}$$

where the locator is now written as

$${}^{r}L^{s}=(\omega-\varepsilon_r-{}^{r}\Sigma_d^{s})^{-1}, \tag{6.5}$$

and where we have approximated $\delta(k-k')$ by -1 in Eq. (6.3) as in Eq. (3.8). We note that the expression for the off-diagonal self-energy Eq. (6.3) has been obtained with the help of the two-component alloy form of Eq. (3.8) and the site-exclusion property given here by

$$\frac{1}{N}\sum_{k,r'',s''}({}^{rr''}M_k^{ss''})({}^{r''r'}G_k^{s''s'})=0, \tag{6.6}$$

because $(1/N)\sum_k V_k=0$, and where we have made use of Eqs. (6.1) and (6.2). Equation (6.4) has been obtained by the use of the two-component alloy form of Eq. (3.3), and the result of comparing two expressions: one is the result of multiplying Eq. (6.1) by V_k and summing over k, r', and s'; the other is the result of multiplying the transpose of Eq. (6.3) by ${}^{r'}x^{s'}$ and summing over r' and s'. Finally, with the use of the identities [Eq. (2.5)] Eq. (6.4) emerges.

Because of the identities of Eq. (2.5), the above EMA reduces to the crystal result when $\varepsilon_A\to\varepsilon_B$. We note that because the pair distribution functions ${}^{BA}g^{ss'}$ and ${}^{AB}g^{ss'}$ of Eq. (2.3) are mixed with respect to the s and s' indices, the full two-component EMA equations which are obtained from solving Eqs. (6.1)–(6.4) involve a 4×4 self-consistent matrix for the self-energies. In the crystal limit these self-energies are nonvanishing. We adopt a two-component matrix notation

$$x^s\equiv\begin{bmatrix} {}^{A}x & 0 \\ 0 & {}^{B}x \end{bmatrix}^s,$$
$$L^s\equiv\begin{bmatrix} {}^{A}L & 0 \\ 0 & {}^{B}L \end{bmatrix}^s, \tag{6.7}$$
$$G_k^{ss'}\equiv\begin{bmatrix} {}^{AA}G & {}^{AB}G \\ {}^{BA}G & {}^{BB}G \end{bmatrix}_k^{ss'}$$

and then a further 2×2 expansion

$$g^{ss'}\equiv(\alpha_s\ \ \beta_s)\begin{bmatrix} g_1 & g_3 \\ g_2 & g_4 \end{bmatrix}\begin{bmatrix} \alpha_{s'} \\ \beta_{s'} \end{bmatrix},$$
$$g_1\equiv\begin{bmatrix} 1 & 0 \\ 0 & 0 \end{bmatrix},\quad g_2\equiv\begin{bmatrix} 0 & 1 \\ 0 & 0 \end{bmatrix},$$
$$g_3\equiv\begin{bmatrix} 0 & 0 \\ 1 & 0 \end{bmatrix},\quad g_4\equiv\begin{bmatrix} 0 & 0 \\ 0 & 1 \end{bmatrix}, \tag{6.8}$$
$$\mathcal{g}\equiv\begin{bmatrix} g_1 & g_3 \\ g_2 & g_4 \end{bmatrix}$$

where α_s and β_s are defined in Eq. (2.4). For the self-energies we have

$$\Sigma_d^s\equiv\begin{bmatrix} {}^{A}\Sigma_d \\ {}^{B}\Sigma_d \end{bmatrix}^s,\quad \Sigma_1^{ss'}\equiv\begin{bmatrix} {}^{AA}\sigma & {}^{AB}\sigma \\ {}^{BA}\sigma & {}^{BB}\sigma \end{bmatrix}^{ss'}. \tag{6.9}$$

For the purposes of obtaining compact expressions for the EMA we next solve the above full alloy equations in a similar way as we did for the split-band limit. We make the ansatz 1,

$$\Sigma_1^{ss'}=(\alpha_s\ \ \beta_s)\begin{bmatrix} \sigma_1 & \sigma_3 \\ \sigma_2 & \sigma_4 \end{bmatrix}\begin{bmatrix} \alpha_{s'} \\ \beta_{s'} \end{bmatrix}, \tag{6.10}$$

and the ansatz 2,

$$G_k^{ss'}=x^sL^s\left[\delta_{ss'}+(\alpha_s\ \ \beta_s)\begin{bmatrix} G_1 & G_3 \\ G_2 & G_4 \end{bmatrix}_k\begin{bmatrix} \alpha_{s'} \\ \beta_{s'} \end{bmatrix}x^{s'}L^{s'}\right]. \tag{6.11}$$

That is, in the end we will have a Green's function of the form of Eq. (6.11) which is easily summed over all components for the total Green's function. We need therefore to find the equations obeyed by the quantities

$$\mathcal{S}\equiv\begin{bmatrix} \sigma_1 & \sigma_3 \\ \sigma_2 & \sigma_4 \end{bmatrix},\quad \Omega_k\equiv\begin{bmatrix} G_1 & G_3 \\ G_2 & G_4 \end{bmatrix}_k. \tag{6.12}$$

We note that each block of Eqs. (6.12) is a 2×2 matrix in the species indices. Once the matrix $\mathcal{S}$ is obtained, we can use Eqs. (6.4) and (6.10) to get all the quantities in Eq. (6.9). When we substitute Eqs. (6.10) and (6.11) and $g^{ss'}$ of Eq. (6.8) into Eq. (6.1), we find that our ansatz 2, Eq. (6.11), is satisfied if Ω_k of Eq. (6.12) obeys the equation

$$\Omega_k=[1-(\mathcal{g}V_k+\mathcal{S})\mathcal{F}]^{-1}(\mathcal{g}V_k+\mathcal{S}) , \tag{6.13}$$

where $\mathcal{g}$ is given in Eq. (6.8) and where $\mathcal{F}$ is given by

$$\mathcal{F}\equiv\begin{bmatrix} F_{20} & F_{11} \\ F_{11} & F_{02} \end{bmatrix}, \quad F_{nm}\equiv\sum_s x^s L^s \alpha_s^n \beta_s^m , \tag{6.14}$$

and where we recall from Eq. (6.7) that each block of $\mathcal{F}$ is a 2×2 matrix. We next substitute Eq. (6.11) and $g^{ss'}$ of Eq. (6.8) into Eq. (6.3) to find that our ansatz 1, Eq. (6.10), is satisfied if $\mathcal{S}$ of Eq. (6.12) obeys the self-consistent equation

$$\mathcal{S}=-\frac{1}{N}\sum_k V_k \mathcal{g}\mathcal{F}\Omega_k , \tag{6.15}$$

which is a 4×4 symmetric matrix. So our work is simplified to solving 10 self-consistent, nonlinear, coupled, algebraic equations. The locators L^s in Eq. (6.14) depend on ${}^r\Sigma_d^s$. These are given by Eq. (6.4) as

$$\begin{aligned}{}^A\Sigma_d^s=-\{&(1-c)[\alpha_s({}^{AA}\sigma_1+{}^{AA}\sigma_3)+\beta_s({}^{AA}\sigma_2+{}^{AA}\sigma_4)] \\ &+c[\alpha_s({}^{AB}\sigma_1+{}^{AB}\sigma_3)+\beta_s({}^{AB}\sigma_2+{}^{AB}\sigma_4)]\} ,\end{aligned} \tag{6.16a}$$

$$\begin{aligned}{}^B\Sigma_d^s=-\{&(1-c)[\alpha_s({}^{BA}\sigma_1+{}^{BA}\sigma_3)+\beta_s({}^{BA}\sigma_2+{}^{BA}\sigma_4)] \\ &+c[\alpha_s({}^{BB}\sigma_1+{}^{BB}\sigma_3)+\beta_s({}^{BB}\sigma_2+{}^{BB}\sigma_4)]\} .\end{aligned} \tag{6.16b}$$

Finally, summing Eq. (6.11) over the environment index s, we obtain the EMA Green's function

$$G_k=\begin{bmatrix} {}^{AA}G & {}^{AB}G \\ {}^{BA}G & {}^{BB}G \end{bmatrix}_k=F_{00}+(F_{10}\ F_{01})\Omega_k\begin{bmatrix} F_{10} \\ F_{01} \end{bmatrix} . \tag{6.17}$$

The total Green's function is obtained by simply summing over the species indices. The EMA equations consist then of Eqs. (6.13) and (6.15)–(6.17) along with the notation Eqs. (6.8), (6.12), and (6.14). The total density of states is given by

$$n(\omega)=-\frac{1}{\pi}\mathrm{Im}({}^AF_{00}+{}^BF_{00}) . \tag{6.18}$$

We note that in the limit $\varepsilon_A\to\infty$, in which case ${}^AL\to0$, the above formulation reduces to the split-band limit of Sec. III.[38] Also, if we arbitrarily set $\mathcal{S}=0$ in Ω_k in Eq. (6.13), then Eq. (6.17) corresponds to the non-self-consistent quasicrystalline approximation (QCA) of Lax,[41] generalized here to include the environment. However, we do not expect the QCA to improve upon the CPA.[38]

B. CPA

The CPA is obtained from the EMA Eqs. (6.1)–(6.5) by letting ${}^{rr'}g^{ss'}\to1$, i.e., no correlation, for which case we assume ${}^r\Sigma_d^s\to\Sigma_d$, ${}^rL^s\to L^r$, ${}^{rr'}\Sigma_1^{ss'}\to\Sigma_1$, and ${}^{rr'}M_k^{ss'}\to M_k$. Since L and M are no longer s dependent, the Green's function Eq. (6.1) is readily summed over s,s' to obtain Eqs. (3.18) and (3.19), except that $\tilde{L}$ is given by

$$\tilde{L}\equiv\frac{1-c}{\omega-\varepsilon_A-\Sigma_d}+\frac{c}{\omega-\varepsilon_B-\Sigma_d} \tag{6.19}$$

with the density of states given by Eq. (3.20). The reduction of the EMA to the CPA has been previously pointed out by Roth.[35,36] Again, if in G_k of Eqs. (3.20) and (6.19) we make the substitution $\Sigma_d=\omega-(\tilde{L}^{-1}+\Sigma)$ the result is the CPA of Soven[1] and Velicky *et al.*[2] Finally, we can show that for the two-component alloy the EMA is related to the virtual-crystal approximation (VCA).[42] It suffices to replace the CPA Σ with ε, the VCA self-energy,[43] to obtain

$$\begin{aligned}&\Sigma_d=\omega-(F_0^{-1}+\varepsilon) , \\ &\varepsilon\equiv(1-c)\varepsilon_A+c\varepsilon_B, \quad F_0\equiv\frac{1}{N}\sum_k(\omega-\varepsilon-V_k)\end{aligned} \tag{6.20}$$

in the CPA equations of Sec. III A.

VII. EMA, A SIMPLIFICATION

Because the full EMA involves solving 10 self-consistent equations, it is reasonable to look for a simplified version of the theory. We first formulate the EMA in a different way.

A. EMA_2

As noted in the preceding section the CPA is obtained from the EMA by taking the pair distribution function ${}^{rr'}g^{ss'}\to1$, i.e., no correlation. We then define a perturbing parameter

$$y_s\equiv\frac{s-cz}{z} \tag{7.1}$$

such that when we take $y_s\to0$ we are taking ${}^{rr'}g^{ss'}\to1$. More specifically, from the averages

$$\frac{1}{c^r}\sum_s {}^rx^s y_s=0, \quad \frac{1}{c^r}\sum_s {}^rx^s y_s^2=\frac{c(1-c)}{z} , \tag{7.2}$$

we see that the functions which involve y_s are small. We then express the pair distribution function of Eq. (6.8) with the help of

$$\alpha_s=1-\frac{y_s}{1-c}, \quad \beta_s=1+\frac{y_s}{c} \tag{7.3}$$

in the equivalent form

$$g^{ss'}=(1\ \ y_s)\begin{bmatrix} g_\alpha & g_\gamma \\ g_\beta & g_\delta \end{bmatrix}\begin{bmatrix} 1 \\ y_{s'} \end{bmatrix}, \quad g_\alpha=\begin{bmatrix} 1 & 1 \\ 1 & 1 \end{bmatrix}, \quad g_\gamma=(g_\beta)^T ,$$

$$g_\beta=\begin{bmatrix} -1/(1-c) & 1/c \\ -1/(1-c) & 1/c \end{bmatrix}, \quad g_\delta=\begin{bmatrix} 1/(1-c)^2 & -1/[c(1-c)] \\ -1/[c(1-c)] & 1/c^2 \end{bmatrix} . \tag{7.4}$$

We next proceed as in Sec. VI for the EMA Eqs. (6.13), (6.15), and (6.16); however, our two ansatzes, 1 and 2, are now

$$\Sigma_1^{ss'}=(1 \quad y_s)\begin{bmatrix}\sigma_\alpha & \sigma_\gamma\\ \sigma_\beta & \sigma_\delta\end{bmatrix}\begin{bmatrix}1\\ y_{s'}\end{bmatrix}, \tag{7.5a}$$

and

$$G_k^{ss'}=x^s L^s\left[\delta_{ss'}+(1 \quad y_s)\begin{bmatrix}G_\alpha & G_\gamma\\ G_\beta & G_\delta\end{bmatrix}_k\begin{bmatrix}1\\ y_{s'}\end{bmatrix}x^{s'}L^{s'}\right]. \tag{7.5b}$$

Letting the 4×4 matrices in Eqs. (7.4), (7.5a), and (7.5b) replace those of Eqs. (6.8), (6.10), and (6.11), we find exactly Eqs. (6.13) and (6.15), but instead of the matrix Eq. (6.14) we now redefine

$$\mathcal{F}\equiv\begin{bmatrix}F_0 & F_1\\ F_1 & F_2\end{bmatrix}, \tag{7.6}$$

and instead of Eqs. (6.17) and (6.14) we now have

$$G_k=\begin{bmatrix}{}^{AA}G & {}^{AB}G\\ {}^{BA}G & {}^{BB}G\end{bmatrix}_k=F_0+(F_0 \quad F_1)\Omega_k\begin{bmatrix}F_0\\ F_1\end{bmatrix},$$
$$F_n\equiv\sum_s x^s L^s y_s^n,\quad {}^rL^s=(\omega-\varepsilon_r-{}^r\Sigma_d^s)^{-1}, \tag{7.7}$$

and the expressions which replace Eq. (6.16) are

$${}^A\Sigma_d^s=-[(1-c)({}^{AA}\sigma_\alpha+y_s\,{}^{AA}\sigma_\beta)+c({}^{AB}\sigma_\alpha+y_s\,{}^{AB}\sigma_\beta)], \tag{7.8a}$$

$${}^B\Sigma_d^s=-[(1-c)({}^{BA}\sigma_\alpha+y_s\,{}^{BA}\sigma_\beta)+c({}^{BB}\sigma_\alpha+y_s\,{}^{BB}\sigma_\beta)]. \tag{7.8b}$$

For the density of states, instead of Eq. (6.18), we now have

$$n(\omega)=-\frac{1}{\pi}\mathrm{Im}({}^AF_0+{}^BF_0). \tag{7.9}$$

B. CPA from EMA$_2$

As we have done previously we take ${}^{rr'}g^{ss'}\to1$, which in the above formulation corresponds to taking $y_s\to0$, and the fact that the only quantities needed are σ_α is easily seen from Eq. (7.8). Also, in the matrix $\mathcal{F}$ in Eq. (7.6) we keep only the quantity F_0. With these assumptions, we perform the matrix operations shown in Eqs. (6.13) and (6.15) with the new definitions Eq. (7.6) to obtain one self-energy for the CPA ($\sigma\equiv\Sigma_1=\sigma_\alpha$),

$$\sigma=({}^AF_0+{}^BF_0)\left[-\frac{1}{N}\sum_k\frac{V_k(V_k+\sigma)}{1-(V_k+\sigma)({}^AF_0+{}^BF_0)}\right], \tag{7.10}$$

which results in ${}^r\Sigma_d^s\to\Sigma_d=-\sigma$ from Eq. (7.8). We see that the functions ${}^rF_n\to{}^rLc^r$, with ${}^rL=(\omega-\varepsilon_r-\Sigma_d)^{-1}$. For the CPA Green's function we get

$$G_k={}^AF_0+{}^BF_0+\frac{({}^AF_0+{}^BF_0)^2(V_k+\sigma)}{1-(V_k+\sigma)({}^AF_0+{}^BF_0)}. \tag{7.11}$$

A very little algebra shows that Eqs. (7.10) and (7.11) give exactly the CPA of Sec. VI B.

C. Simplified EMA (SEMA)

We note from the work of the preceding subsection that the CPA involves the quantity F_0 in Eqs. (7.6) and (7.7), and that the reason for this is that in the CPA limit the locators from Eq. (7.7) are no longer dependent on the index s; furthermore, because of Eq. (7.2) the functions which involve the parameter y_s in the EMA above will be small. We therefore consider the approximation of keeping only the F_0 functions in the EMA of Sec. VII A and still going beyond the CPA to include the environment contribution through Eq. (7.8). Specifically, we then have

$$G_k={}^AF_0+{}^BF_0+({}^AF_0 \quad {}^BF_0 \quad 0 \quad 0)\Omega_k\begin{bmatrix}{}^AF_0\\ {}^BF_0\\ 0\\ 0\end{bmatrix}, \tag{7.12}$$

where the rest of the equations are

$$\Omega_k=[1-(\mathcal{g}V_k+\mathcal{S})\mathcal{F}]^{-1}(\mathcal{g}V_k+\mathcal{S}),$$
$$\mathcal{S}=-\frac{1}{N}\sum_k V_k\mathcal{g}\mathcal{F}\Omega_k,$$
$$\mathcal{F}=\begin{bmatrix}F_0 & 0\\ 0 & 0\end{bmatrix},\quad {}^rF_0=\sum_s {}^rx^s\,{}^rL^s,$$
$${}^rL^s=(\omega-\varepsilon_r-{}^r\Sigma_d^s)^{-1} \tag{7.13}$$

with $\mathcal{g}$, $\mathcal{S}$, and Ω_k as written in Eqs. (7.4), (7.5a), and (7.5b), and ${}^r\Sigma_d^s$ as in Eqs. (7.8a) and (7.8b). After carrying out the complete matrix operations one self-energy equation is found for $\sigma\equiv\sigma_\alpha$, similar to Eq. (7.10), but where the ${}^rF_0$ function involves an s-dependent locator. The diagonal self-energy ${}^s\Sigma_d$ depends also on σ_β which is finite and is given in terms of σ_α. Because in the split-band limit the above equations are much simpler, we looked at the moments in this limit and found that the above approximation actually conserves one more moment than the previous EMA of Sec. III. However, we also studied the analytic properties of the above approximation in the split-band limit to find that the ${}^rF_0$ functions that appear in the only resulting self-energy of this approximation have a pole in the $s=0$ term (for the $\varepsilon_A\to\infty$ case), which is responsible for nonanaliticities. These problems persist in the numerical calculation for the full two-component system. To remedy this situation we add back small terms involving ${}^rF_1$ of Eq. (7.7). That is, we make the replacement

$${}^rF_0\to{}^r\tilde{F}_1, \tag{7.14}$$

where

$$ {}^{A}\tilde{F}_1=\sum_s {}^{A}x^s\,{}^{A}L^s\left[1-\frac{y_s}{1-c}\right], $$
$$ {}^{B}\tilde{F}_1=\sum_s {}^{B}x^s\,{}^{B}L^s\left[1+\frac{y_s}{c}\right], \tag{7.15} $$

since the $s=0$ (or $s=z$ in the case of $\varepsilon_B\to\infty$) pole is not a problem for ${}^{r}\tilde{F}_1$ in Eqs. (7.12) and (7.13). This completes the simplified EMA (SEMA). The CPA results when we neglect the parameter y_s completely. Summarizing the SEMA equations, the total Green's function[38] is

$$ G_k={}^{A}F_0+{}^{B}F_0+\frac{({}^{A}\tilde{F}_1+{}^{B}\tilde{F}_1)^2(V_k+\sigma)}{1-({}^{A}\tilde{F}_1+{}^{B}\tilde{F}_1)(V_k+\sigma)}, \tag{7.16} $$

where we have only one self-energy

$$ \sigma=-\frac{1}{N}\sum_k V_k\frac{({}^{A}\tilde{F}_1+{}^{B}\tilde{F}_1)(V_k+\sigma)}{1-({}^{A}\tilde{F}_1+{}^{B}\tilde{F}_1)(V_k+\sigma)}, \tag{7.17} $$

and the diagonal self-energy in the locator of Eq. (7.13) is given by

$$ {}^{r}\Sigma_d^s\to\Sigma_d^s=-\sigma\left[1+\frac{{}^{B}\tilde{F}_1/c-{}^{A}\tilde{F}_1/(1-c)}{{}^{A}\tilde{F}_1+{}^{B}\tilde{F}_1}y_s\right]. \tag{7.18} $$

Finally, the total density of states is given by

$$ n(\omega)=-\frac{1}{\pi}\mathrm{Im}({}^{A}F_0+{}^{B}F_0). \tag{7.19} $$

VIII. SEMA MOMENTS AND ANALYTIC PROPERTIES, SPLIT-BAND LIMIT

The split-band limit for SEMA is obtained from Eqs. (3.12)–(3.16) by making the replacement $F_2\to F_1\equiv{}^{B}\tilde{F}_1$. The moments in the split-band limit for SEMA can be studied by the procedure explained in Sec. IV. These are given in Table I. The SEMA improves upon the moments of the previous EMA of Sec. III by conserving one more moment. The error in the EMA moments involves a term similar to the y_s^2 term in Eq. (7.2), which is apparently neglected in the SEMA, suggesting that the SEMA treats the $1/z$ terms more consistently.

SEMA is also analytic in the limit $\varepsilon_A\to\infty$, $\varepsilon_B\equiv 0$. To show this the self-energy σ of Eq. (7.17) can be rearranged to give

$$ \frac{1}{N}\sum_k\frac{V_k}{1-{}^{B}\tilde{F}_1(V_k+\sigma)}=0. \tag{8.1} $$

This equation can be further rearranged to obtain a self-consistent expression similar to Eq. (4.1) given by

$$ {}^{B}\tilde{F}_1=\frac{1}{N}\sum_k\frac{1}{({}^{B}\tilde{F}_1)^{-1}-\sigma-V_k}. \tag{8.2} $$

The condition which determines analyticity here, given a first guess for σ with a positive imaginary part, is that in Eq. (8.2) the inequality

$$ \mathrm{Im}[({}^{B}\tilde{F}_1)^{-1}-\sigma]\geq 0,\quad {}^{B}\tilde{F}_1=\sum_s B_x^s\,{}^{B}L^s\beta_s,\quad \beta_s=1+\frac{y_s}{c} \tag{8.3} $$

be satisfied. We find that because

$$ |{}^{B}\tilde{F}_1|^2=\left|\sum_s\frac{{}^{B}x^s\beta_s}{\omega-\sigma\beta_s}\right|^2\leq c\sum_s{}^{B}x^s\left|\frac{\beta_s}{\omega-\sigma\beta_s}\right|^2 \tag{8.4} $$

and since the imaginary part of $({}^{B}\tilde{F}_1)^{-1}$ is given by

$$ \mathrm{Im}[({}^{B}\tilde{F}_1)^{-1}]=\frac{\sigma''\sum_s{}^{B}x^s|\beta_s/(\omega-\sigma\beta_s)|^2}{|{}^{B}\tilde{F}_1|^2}, \tag{8.5} $$

where σ'' is the imaginary part of σ, then the inequality Eq. (8.3) is always satisfied in the SEMA for this limit.

IX. IMPURITY EQUATION, FULL ALLOY

A. CPA and EMA

The impurity equations for the full two-component alloy are an obvious extension of Eqs. (5.3) and (5.4) for the CPA and the EMA, respectively. For the EMA we see that we can obtain the environment levels for each possible configuration s of the impurity nearest neighbors. Each level is weighted according to the probability of the configuration.[33] To determine these energy levels in SEMA we only need one self-energy from Eq. (7.18).

B. Virtual-crystal approximation (VCA)

To reduce our result to the VCA limit we replace the CPA expression for Σ_d of Eq. (5.3) by the expressions in Eq. (6.20) to obtain the local density of states for the impurity ε_C,

$$ n(\omega)=-\frac{1}{\pi}\mathrm{Im}(\varepsilon-\varepsilon_C-F_0^{-1})^{-1}, \tag{9.1} $$

with ε and F_0 defined in Eq. (6.20). Again the energy at which the pole occurs corresponds to the impurity energy level.[32,38] An extension of Eq. (9.1) to more realistic systems such as semiconductor alloys results in a condition for finding impurity energy levels which is of the same form as the Hjalmarson *et al.* impurity equation.[44] In the crystal limit $\varepsilon_A=\varepsilon_B$ Eq. (9.1) gives the Koster-Slater condition[39] for an impurity in a crystal host.

X. PERTURBATION APPROACH TO ENVIRONMENT LEVELS

As mentioned in the Introduction there are several methods available to obtain environment levels as in the work of Myles and Dow,[32] Ford and Myles,[33] as well as the method of Mariette,[45] and the method of the present work. We would like to investigate the possibility of an alternate simple method.

We assume we have a VCA host alloy medium with the Hamiltonian

$$ H_0=\sum_p|p\rangle\varepsilon\langle p|+\sum_{\substack{p,q\\ p\neq q}}|p\rangle V_{pq}\langle q|, \tag{10.1} $$

where ε is the VCA diagonal energy. We consider the perturbation H_1,

$$ H_1=u_0|0\rangle\langle 0|,\quad u_0=\varepsilon_C-\varepsilon, \tag{10.2} $$

that is we have a defect at the zeroth site. Following the standard procedure from the review of Pantelides,[46] the equation for the bound state due to the impurity is given by

$$u_0=[G^0_{00}(E_b)]^{-1} . \tag{10.3}$$

This last equation when satisfied gives the position of the bound state E_b due to the defect potential.[46] We consider next a perturbation H_2

$$H_2=\sum_{i(\neq 0)}(\varepsilon_i-\varepsilon)\,|\,i\,\rangle\langle\,i\,|\ , \tag{10.4}$$

which is designed to take into account the local environment fluctuations about the VCA medium. The energy shift of the impurity level obtained in Eq. (10.3) due to the different impurity neighbor possibilities is then to lowest order

$$\Delta E=\frac{\langle\,\psi_c\,|\,H_2\,|\,\psi_c\,\rangle}{\langle\,\psi_c\,|\,\psi_c\,\rangle}\ , \tag{10.5}$$

where $|\,\psi_c\,\rangle$ is the impurity wave function. Evaluating this expression with the use of H_2 of Eq. (10.4) and restricting the sum to nearest neighbors, we find

$$\Delta E_s=\frac{|\,G^0_{10}(E_b)\,|^2}{\sum_i |\,G^0_{i0}\,|^2}[s\varepsilon_A+(z-s)\varepsilon_B]\ , \tag{10.6}$$

which are the split levels of the impurity due to the local environment, one for each possible neighbor configuration, arising from the perturbation H_2 above. Equation (10.6) assumes that we know the impurity bound state from Eq. (10.3).

XI. SHORT-RANGE ORDER

In this section we deal with the inclusion of short-range order in the sense of nonrandom correlations. We follow an approach similar to that of Jacobs,[20] and Zin and Stern,[25] who study this property through a short-range-order parameter. The technique of Zin and Stern is correct in the clustering limit; however, their work does not yield the correct result in the perfect ordering limit. We include the short-range-order property in the EMA by modifying not only the concentration of sites from Eq. (2.2), but also the pair distribution functions of Eq. (2.3). The EMA which we discuss below gives the exact results in the clustering as well as perfect order limits.[25]

We define $P_{rr'}$ as the probability of finding an r' atom as a nearest neighbor to an r atom. It is given by[25]

$$\begin{aligned} &P_{AA}=1-c(1+\gamma),\quad P_{AB}=c(1+\gamma)\ ,\\ &P_{BA}=(1-c)(1+\gamma),\quad P_{BB}=1-(1-c)(1+\gamma) \end{aligned} \tag{11.1}$$

in terms of the short-range-order parameter γ which takes on the range of values

$$\gamma=\begin{cases} -1 & \text{clustering}\\ 0 & \text{randomness}\\ 1, & c=0.5\ \text{ perfect order}\ . \end{cases} \tag{11.2}$$

The short-range-order parameter cannot be chosen arbitrarily; its range depends on the concentration of species through the condition that the $P_{rr'}$ remain positive.[25] The concentration of B and A sites with s B neighbors is now given by

$$\begin{aligned} {}^Bx^s&=\begin{bmatrix} z\\ s\end{bmatrix}(P_{BA})^{z-s}(P_{BB})^s c\ ,\\ {}^Ax^s&=\begin{bmatrix} z\\ s\end{bmatrix}(P_{AB})^s(P_{AA})^{z-s}(1-c)\ , \end{aligned} \tag{11.3}$$

and the pair distribution functions become

$$\begin{aligned} &{}^{AA}g^{ss'}=\alpha_s\alpha_{s'}h_{AA},\quad {}^{AB}g^{ss'}=\beta_s\alpha_{s'}h_{AB}\ ,\\ &{}^{BA}g^{ss'}=\alpha_s\beta_{s'}h_{BA},\quad {}^{BB}g^{ss'}=\beta_s\beta_{s'}h_{BB}\ , \end{aligned} \tag{11.4a}$$

where

$$h_{AA}=\frac{1-c}{P_{AA}},\quad h_{AB}=\frac{c}{P_{AB}},\quad h_{BA}=\frac{1-c}{P_{BA}},\quad h_{BB}=\frac{c}{P_{BB}}\ , \tag{11.4b}$$

and where α_s and β_s are given in Eq. (2.4). We also have the identities

$$\frac{1}{c^r}\sum_s {}^rx^s=1,\quad \sum_{s'r'} {}^{rr'}g^{ss'}\,{}^{r'}x^{s'}=1\ . \tag{11.5}$$

A. EMA, short-range order

In order to incorporate short-range order into the EMA, we simply replace the nearest-neighbor pair distribution function of Eqs. (6.2) and (2.3) by the correlated version of Eq. (11.4). We still make the approximation ${}^{rr'}\Delta^{ss'}(k-k')=-1$ in Eq. (6.3). The term which we neglect could play an important role when we consider the effects of short-range order and not the local environment, since the nearest-neighbor part of Δ no longer vanishes in the limit of averaging out the environment when nonrandom correlations are included, in contrast to the case of random correlations when ${}^{rr'}g^{ss'}\to 1$ in the CPA limit.

The EMA which results when we consider short-range order is very similar to the EMA of Sec. VI, Eqs. (6.13)–(6.16), but with the matrices of Eq. (6.8) now given by

$$\begin{aligned} g_1&=\begin{bmatrix} h_{AA} & 0\\ 0 & 0\end{bmatrix},\quad g_2=\begin{bmatrix} 0 & h_{AB}\\ 0 & 0\end{bmatrix}\ ,\\ g_3&=\begin{bmatrix} 0 & 0\\ h_{BA} & 0\end{bmatrix},\quad g_4=\begin{bmatrix} 0 & 0\\ 0 & h_{BB}\end{bmatrix}\ . \end{aligned} \tag{11.6}$$

We use a modified ansatz of the form

$$\sigma_i(\text{new})=h_i\sigma_i(\text{old}),\quad G_{ki}(\text{new})=h_iG_{ki}(\text{old}) \tag{11.7}$$

involving the h's from Eq. (11.4), and old refers to the previous ansatz of Sec. VI. The diagonal self-energies of Eq. (6.16) are now given by

$$ {}^{A}\Sigma_d^s = -[\alpha_s(P_{AA}\,{}^{AA}\sigma_1 + P_{BA}\,{}^{AA}\sigma_2 + P_{AB}\,{}^{AB}\sigma_1 + P_{BB}\,{}^{AB}\sigma_2) + \beta_s(P_{AA}\,{}^{AA}\sigma_3 + P_{BA}\,{}^{BA}\sigma_4 + P_{AB}\,{}^{AB}\sigma_3 + P_{BB}\,{}^{BB}\sigma_4)] , \tag{11.8a} $$

$$ {}^{B}\Sigma_d^s = -[\alpha_s(P_{AA}\,{}^{BA}\sigma_1 + P_{BA}\,{}^{BA}\sigma_2 + P_{AB}\,{}^{BB}\sigma_1 + P_{BB}\,{}^{BB}\sigma_2) + \beta_s(P_{AA}\,{}^{BA}\sigma_3 + P_{BA}\,{}^{BA}\sigma_4 + P_{AB}\,{}^{BB}\sigma_3 + P_{BB}\,{}^{BB}\sigma_4)] . \tag{11.8b} $$

The above expressions are very helpful because they make it possible to see which σ's vanish when certain limits are considered. We find that for the case of $\gamma=-1$ the EMA Green's function reduces to the exact clustering result[38]

$$ G_k = \frac{(1-c)L_A}{1-V_kL_A} + \frac{cL_B}{1-V_kL_B} . \tag{11.9a} $$

For the case of $\gamma=1$, $c=0.5$ the EMA Green's function reduces to the exact perfect-ordering result[38]

$$ G_k = \frac{\omega-(\varepsilon_A+\varepsilon_B)/2+V_k}{(\omega-\varepsilon_B)(\omega-\varepsilon_A)-V_k^2} . \tag{11.9b} $$

The density of states is given by

$$ n(\omega) = -\frac{1}{\pi}\mathrm{Im}\left[\frac{1}{N}\sum_k G_k\right] . \tag{11.10} $$

B. CPA with short-range order

Using the EMA formalism, it is possible to obtain a CPA which incorporates short-range order. In Sec. VI we obtained the CPA by taking ${}^{rr'}g^{ss'}\to 1$, i.e., no correlation since the CPA sees an average random environment. We make a similar step here by averaging out the effects of the environment in the pair distribution function with short-range order of Eq. (11.4). We make use of the expressions

$$ \frac{1}{c}\sum_s {}^{B}x^s{}_S = zP_{BB}, \quad \frac{1}{(1-c)}\sum_s {}^{A}x^s{}_S = zP_{AB} \tag{11.11} $$

to obtain

$$ g^{AA} = \frac{P_{AA}}{1-c}, \quad g^{AB} = \frac{P_{AB}}{c}, \quad g^{BA} = \frac{P_{AB}}{1-c}, \quad g^{BB} = \frac{P_{BB}}{c} . \tag{11.12} $$

These pair distribution functions are used to obtain the 2×2 correlated CPA. The EMA equations are simply Eqs. (6.1)–(6.5) with the environment indices s,s' omitted. The solution for the correlated Green's function is

$$ G_k = \begin{bmatrix} G^{AA} & G^{AB} \\ G^{BA} & G^{BB} \end{bmatrix}_k = \begin{bmatrix} d^{BB}x^AL^A & -d^{AB}x^BL^B \\ -d^{BA}x^AL^A & d^{AA}x^BL^B \end{bmatrix}\frac{1}{\mathcal{D}} , \tag{11.13} $$

where

$$ \begin{aligned} d^{rr'} &= \delta_{rr'} - x^rL^r(V_kg^{rr'}+\sigma^{rr'}) , \\ \mathcal{D} &= d^{AA}d^{BB} - d^{AB}d^{BA} , \\ L^r &= (\omega-\varepsilon_r-\Sigma_d^r)^{-1} , \end{aligned} \tag{11.14} $$

and the self-energies are given by

$$ \sigma^{rr'} = -\frac{1}{N}\sum_k V_k \sum_{r''} g^{rr''}G_k^{r''r'}(L^{r'}X^{r'})^{-1} , \tag{11.15} $$

and the diagonal self-energies needed for the locators Eq. (11.14) are given by

$$ \Sigma_d^r = -\sum_{r'}\sigma^{rr'}x^{r'} . \tag{11.16} $$

This completes the correlated CPA equations. We note that in the limit $g^{rr'}\to 1$ we obtain the CPA of Sec. VI. We also note that the above formulation reduces to the exact clustering and perfect ordering limits Eqs. (11.9a) and (11.9b), respectively. Our results bear some resemblance to the work of Jacobs.[20]

XII. MOMENTS OF CORRELATED CPA SPLIT-BAND LIMIT

We have investigated the moments of the above approximation in the split-band limit. These are given in Table I. We see that the second moment deviates from the exact result explained in Sec. IV. We attribute this early deviation of the moments to the approximation made in Eq. (6.3) of neglecting the second term in ${}^{rr'}\mathcal{A}^{ss'}(k-k')$. Further investigation in this matter needs to be carried out.

XIII. RESULTS

Our calculations in this work have been performed for the simple-cubic system with nearest-neighbor interactions. Integrals which appear, for example, in Eqs. (3.14), (6.15), (7.17), and (11.10) have been carried out with the use of the density of states for the simple-cubic tight-binding model of Jelitto,[47] for which

$$ V_k = -2t[\cos(k_xa)+\cos(k_ya)+\cos(k_za)] , $$

and we take $t=0.5, a=1.0$.

A. Split-band limit ($\varepsilon_A\to\infty$, $\varepsilon_B\equiv 0.0$)

In Fig. 1 we compare the CPA and EMA results in the split-band limit. Figure 1(a) shows the density of states for concentration $c=0.5$ and impurity level with impurity $\varepsilon_C=3.2$ in the CPA. We use Eq. (3.20) to find the density of states, while to find the impurity level we use Eq. (5.3), i.e., the zero of $\omega-\varepsilon_C-\Sigma_d$. Figure 1(b) shows the density of states and the environment impurity levels for each configuration s of the nearest neighbors using the EMA and the parameters as in Fig. 1(a). We use Eq. (3.17) for the density of states, and Eq. (5.4) for the impurity levels, i.e., the zeros of $\omega-\varepsilon_C-\Sigma_d^s$. We note that the EMA band is wider than the CPA band

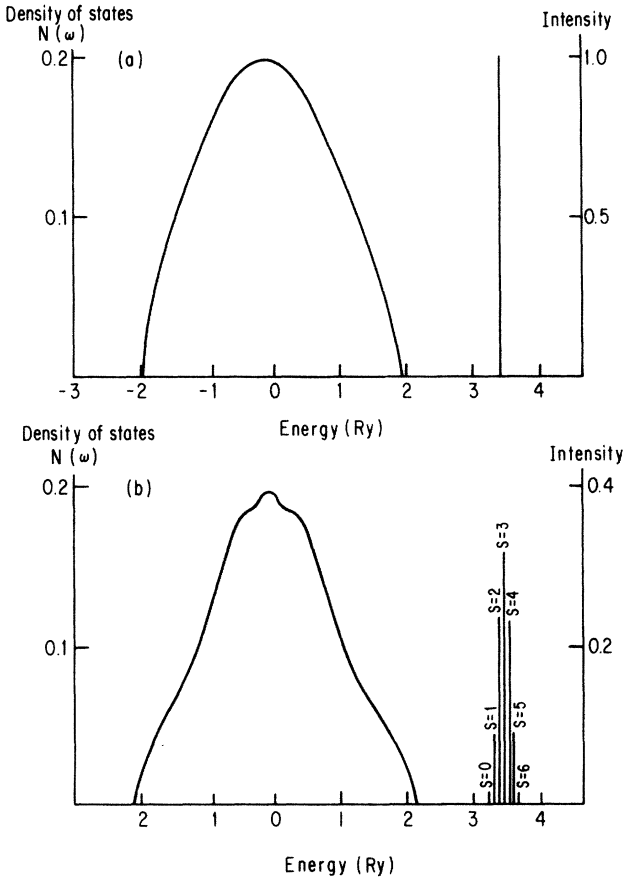

FIG. 1. Split-band-limit density of states and impurity level for concentration $c=0.5$, and impurity orbital energy $\varepsilon_C=3.2$. (a) The CPA using Eq. (3.20) for the density of states, and Eq. (5.3) for the impurity. (b) The EMA using Eq. (3.17) for the density of states and Eq. (5.4) for the impurity.

due to the possibility of having a B atom surrounded by six B atoms. The center peak in the EMA corresponds to the possibility of a B atom surrounded by six A atoms. We have broadened the center peak independently of the rest of the band. Seven impurity levels are obtained in the EMA because the impurity samples seven possible nearest-neighbor configurations. Each possibility gives rise to a level. The height of the line for each level has been weighted according to its probability of occurrence[32,33,45] with the use of the binomial distribution given in Eq. (5.4). The CPA band, on the other hand, gives an average band since this approximation averages the environment. There is only one impurity level in the CPA which occurs at the most probable configuration, $s=3$. Figure 2 shows the partial density of states obtained in the EMA using a decomposition of Eq. (3.17) according to Eq. (3.11) for the host band of Fig. 1(b), corresponding to environment configurations of $s=0$ to $s=6$ B neighbors.

B. Full two-component alloy

Figure 3(a) shows the density of states using the two-component alloy approximations for the CPA using Eq. (3.20) with Eq. (6.19), and for the SEMA using Eq.

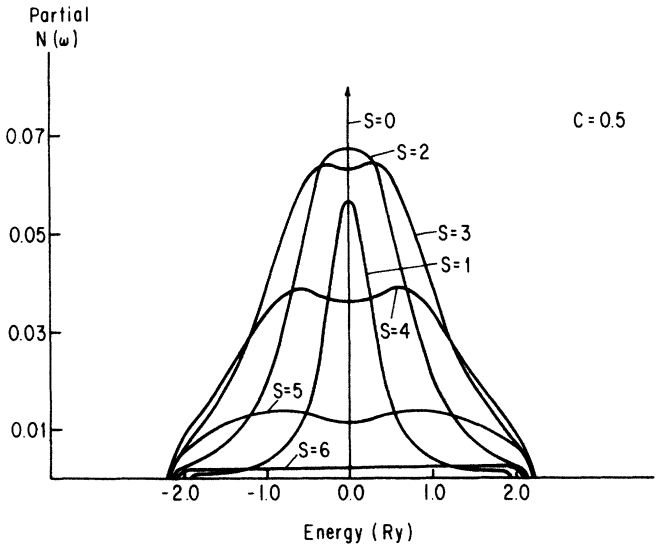

FIG. 2. Partial density of states for each configuration s of the B neighbors with $c=0.5$ for the EMA using Eqs. (3.11) and (3.17).

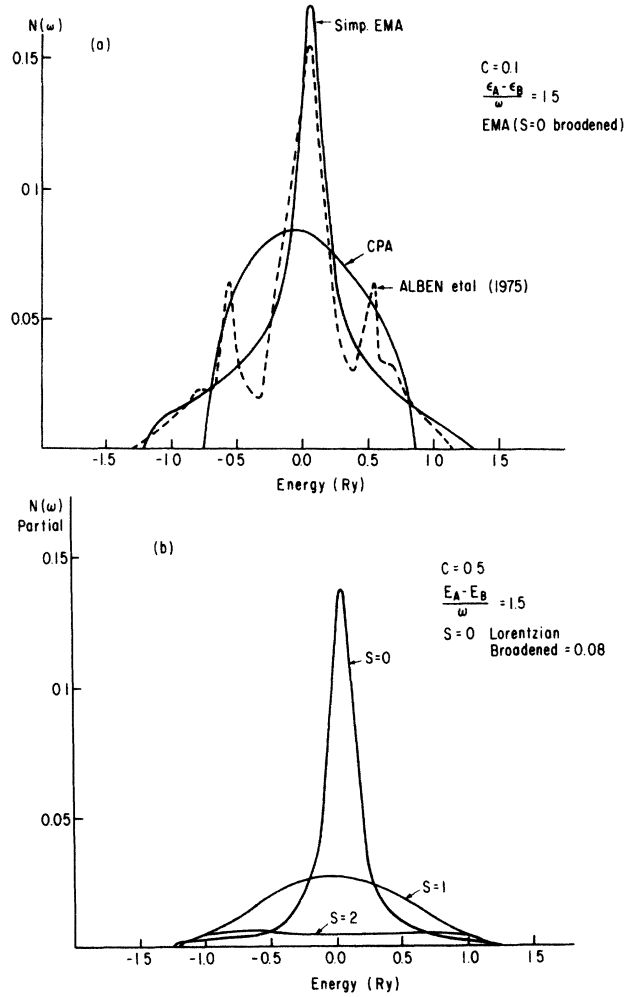

FIG. 3. (a) Comparison of the density of states from the work of Alben *et al.* with the CPA of Eqs. (3.20) and (6.19), and the SEMA from Eq. (7.19) for $c=0.1$, and $\varepsilon_A-\varepsilon_B=1.5$. (b) Partial density of states for the SEMA of (a) using Eqs. (7.15) and (7.19).

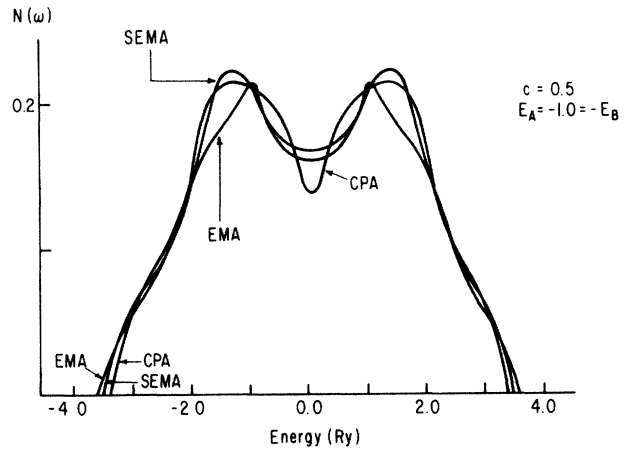

FIG. 4. Comparison between the CPA and the SEMA and the EMA for $c=0.5$, $\varepsilon_A=-\varepsilon_B=-1$.

(7.19). We compare with the exact results of Alben *et al.*[9] for the concentration $c=0.1$ and scattering strength $\varepsilon_A-\varepsilon_B=1.5$, the parameters used in that work. We see that the EMA results are very good compared to the exact results in that there are wings on the density of states; however, the satellite structure (side peaks) associated with pairs[48] is not resolved. The CPA as mentioned above gives an average structure.[9] The reason for the good agreement of the EMA with the exact results is seen in Fig. 3(b), where the partial density of states is shown by means of Eqs. (7.15) and (7.19). We see that the center peak corresponds to the one-site contribution to the total density of states. We also observe that our SEMA gives a smooth curve for the $s=1$ B neighbor partial density of states, and a wider curve for $s=2$ B neighbor, etc. This shows how tails in the density of states arise from local effects. Figure 4 shows a density of states comparison for the CPA, the EMA, and the SEMA for concentration $c=0.5$, $\varepsilon_A=-\varepsilon_B=-1$. In Fig. 4 we show the well-known CPA results;[43] in our work we use Eqs. (3.20) and (6.19). We know from the work of Alben *et al.*[9] that the CPA does not quite account for the correct gap or the correct bandwidth of the alloy for parameters in this range. Figure 4 shows the full self-consistent EMA [Eq. (6.18)] which involves ten self-consistent equations [Eq. (6.15)]. We note that the EMA has improved on the onset of gap opening over the CPA as well as being broader and having more structure. The two small peaks occur at the positions of the orbital energies of the two alloy components. Figure 4 shows the SEMA using Eq. (7.19), and it is as easy to evaluate as is the CPA. We see that there is good agreement with the full EMA concerning the breadth of the band as well as the gap. However, there is disagreement with the position of the two peaks, and SEMA actually seems closer to the exact results of Alben *et al.*[9] These results are similar to those of Browers *et al.*[11] in their Bethe-Peierls approximation.

Concerning the impurity results in the two-component alloy system, Table II shows the SEMA impurity environment levels calculated using Eq. (5.4) and the formulation of Sec. VII C compared with those obtained using the perturbation approach to the impurity environment levels of Eq. (10.6) and Eq. (10.3) in the VCA host. The impurity levels are for an impurity orbital energy placed near the host band edge shown in the table. We see that for the parameters chosen the perturbational approach is in very good agreement with the more-sophisticated results of SEMA. On the other hand, the VCA cannot be used for the strong scattering regime[49–51] and it is necessary to use the more-sophisticated EMA approach for example when the bands are split. Figure 5 shows the results of SEMA using Eq. (5.4) with the formulation of Sec. VII C for a concentration of $c=0.5$. Three calculations are shown for impurity orbital energies to the far left, $\varepsilon_C=-6.5$, to the far right, $\varepsilon_C=6.5$, and the alloy gap $\varepsilon_C=0.0$. The host orbital energies are $\varepsilon_A=-3.5=-\varepsilon_B$. In all cases we notice that the impurity levels due to six B neighbors are furthest away from the B host band, and similarly for the case of the A host band. This is probably due to the quantum-mechanical repulsion of levels. We further note that the splitting of the impurity levels in the gap is greater than that of the band edges. The results for this case are qualitatively similar to those of Myles and Dow[32] for a one-dimensional alloy, though the latter includes further small splittings due to farther neighbors.

For the case of short-range order with nonrandom correlation we have seen that the EMA and the correlated CPA both reduce to the exact results of Eqs. (11.9). It is helpful to get some idea of the effects of varying the parameter γ in the work of Sec. XI for the EMA. We do this for the split-band limit for concentration $c=0.5$; the randomness correlation case $\gamma=0$ is shown in Fig. 6; the clustering regime $\gamma=-0.9$ is shown in Fig. 6; and the near-perfect-ordering regime $\gamma=0.9$ is shown in Fig. 6. The random case is the same as in Fig. 1(b), but this time we do not insert broadening so that we can compare with the other two cases. The sharp peak corresponds to the $s=0$ B neighbors, and in the case of clustering the short-range order does away with the sharp peak and the band is totally broadened to its maximum, showing that a nearly pure B environment is present, since the B species segregates. In the case of close to

TABLE II. Comparison of the results for the SEMA impurity levels Eq. (5.4) using the formulation of Sec. VII C with those using the perturbational result Eqs. (10.3) and (10.6) in VCA. The impurity orbital energies are near the band edge as shown.

	ε_A	ε_B	c	ε_C	Level	$s=0$	$s=1$	$s=2$	$s=3$	$s=4$	$s=5$	$s=6$	Band edges
EMA	−0.5	0.5	0.5	3.8		4.17	4.19	4.21	4.22	4.24	4.26	4.27	−3.25–3.25
VCA	−0.5	0.5	0.5	3.8	4.22	4.16	4.18	4.20	4.22	4.23	4.25	4.27	−3.00–3.00

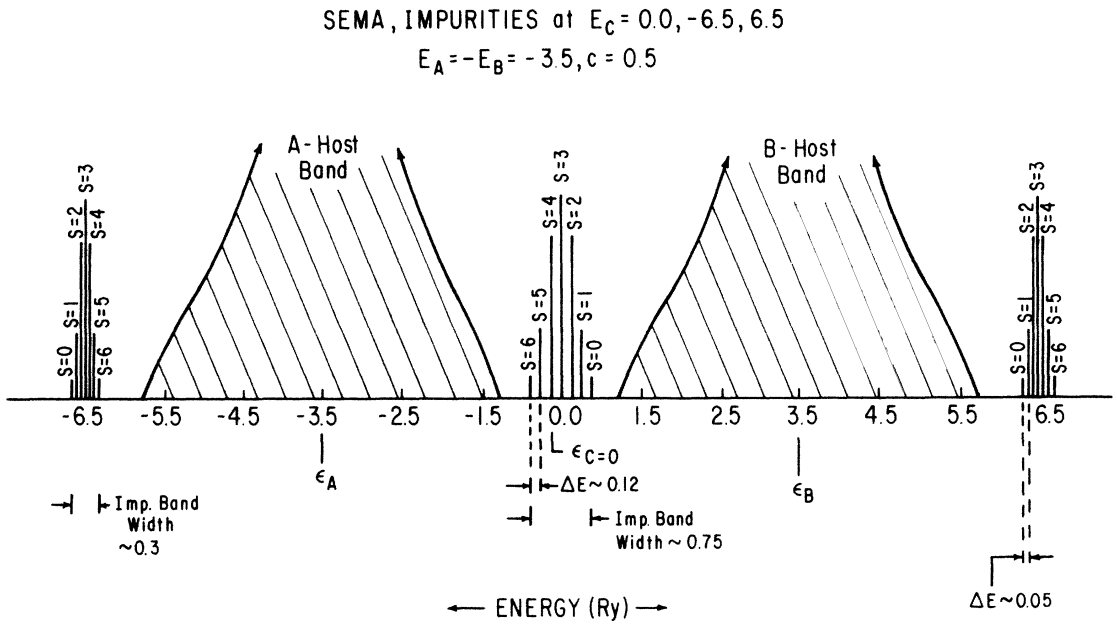

FIG. 5. Impurity levels using the SEMA Eqs. (7.19) and (5.4), with the formulation of Sec. VII C for $c = 0.5$, $\varepsilon_A = -3.5 = -\varepsilon_B$, and $\varepsilon_C = 0.0, -6.5, 6.5$.

perfect order the short-range order shrinks the band and the sharp peak is more emphasized. We recall that in this case we have one B atom surrounded by six A atoms so that the shape of the band indicates a depletion of B neighbors to the B site. Finally, in Fig. 7 we show the results of evaluating Eqs. (11.9) and (11.10) for clustering and perfect order for a concentration $c = 0.5$. In Fig. 7(a) we use $\varepsilon_A = -\varepsilon_B = -3.5$, and in Fig. 7(b) we use $\varepsilon_A = -\varepsilon_B = -1.0$. In both of these cases we see clearly the effects of segregation; the band shape is a simple addition of the density of states of two shifted crystal bands weighted by their concentrations. Figure 7(c) is the exact perfect ordering result for $\varepsilon_A = -\varepsilon_B = -1.0$. We see that there is always a band gap in this system, and the gap persists until the orbital energies of the two species match.

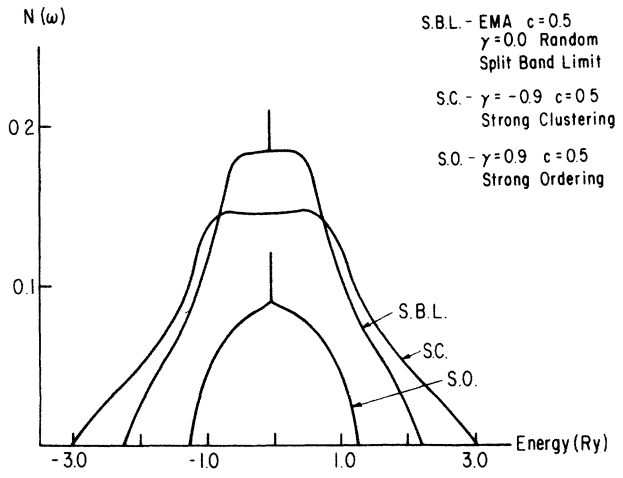

FIG. 6. The EMA density of states using the formulation of Sec. XI for short-range order in the split-band limit $\varepsilon_A \to \infty$, $c = 0.5$, and $\varepsilon_B = 0.0$ for the limits $\gamma = 0.0, -0.9$, and 0.9.

XIV. CONCLUSION

We have made a study of the local environment effects using the single-site effective medium approximation (EMA),[35–37] which is a natural extension of the single-site coherent-potential approximation[1,2] (CPA) to include short-range order. We have developed a self-consistent consistent EMA formalism which treats the two-component random alloy including environment effects. A simplified version of the EMA (SEMA) has been obtained, which is as easy to work with as is the CPA. The agreement with the exact results of Alben *et al.*[9] is improved over the CPA concerning the width of the band and the onset of the gap.

When an impurity is introduced in the host alloy system, it experiences the environmental fluctuations of the random alloy. This gives rise to a set of impurity levels characteristic of the nearest-neighbor alloy configurations in contrast to the one level obtained using the CPA. By making a perturbation about the virtual-crystal approximation (VCA) a simple scheme which models the splitting of impurity levels due to the environment effects is obtained. This simple scheme gives very good results when compared with the above SEMA in the VCA limit.

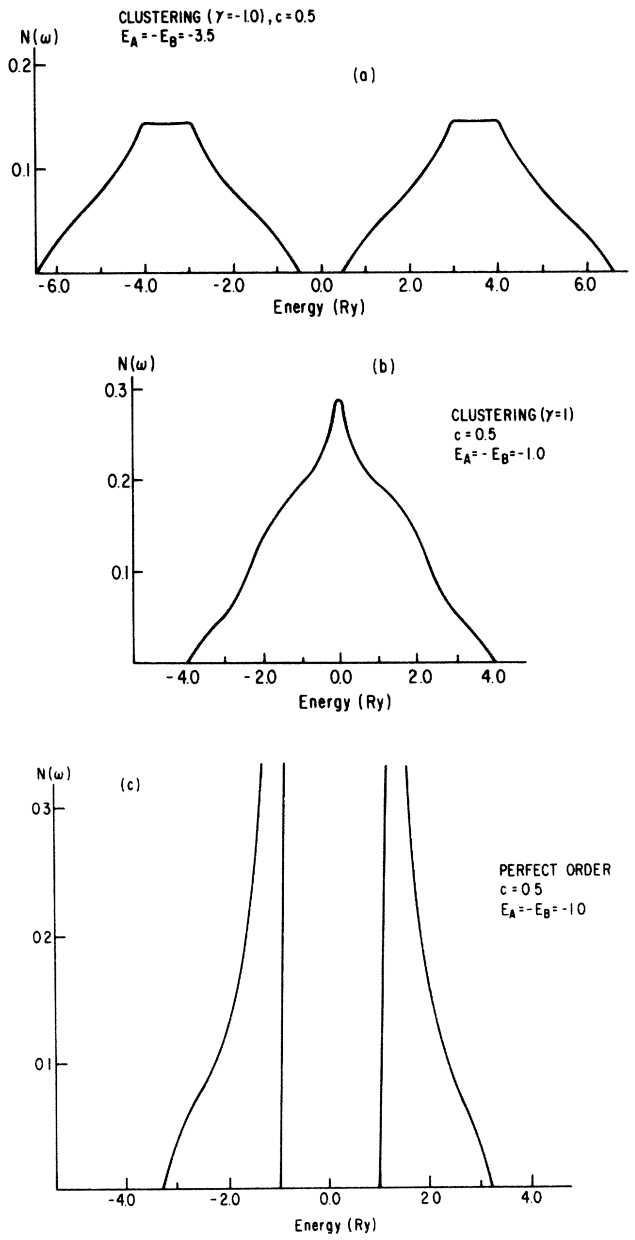

FIG. 7. Exact-clustering and perfect-ordering results of Eqs. (11.9) and (11.10) for $c=0.5$. (a) $\gamma=-1.0$, $\varepsilon_A=-\varepsilon_B=-3.5$ (clustering). (b) $\gamma=-1.0$, $\varepsilon_A=-\varepsilon_B=-1.0$ (clustering). (c) $\gamma=1.0$, $\varepsilon_A=-\varepsilon_B=-1.0$ (perfect ordering).

We have also considered the effects of short-range order with nonrandom correlations using the EMA, and find that it gives the exact results of clustering and perfect-ordering limits. An extension of the CPA which includes short-range order has been developed which reduces to the exact-clustering and perfect-ordering limits as well. However, this approach needs further investigation, since it is possible to improve the moments of Sec. XII above by taking the k-dependent part of $\Delta(k-k')$ into account.

Comparing this theory with other work the most-relevant method to discuss is the embedded-cluster method.[32] Our theory gives a self-consistently determined effective medium which models the local environment by including the concentration of species in the neighbor shell. The embedded-cluster method includes more detail such as the configuration of the neighbor shell and in simple cases, higher neighbors, but is more difficult to apply and does not have a self-consistent translationally invariant medium. The results appear to be quite comparable however. It is reasonable to expect that the neighbor shell gives the greatest effect,[31] although it would be worthwhile to study under what conditions the levels are further broadened by higher neighbor effects.[33]

The above theory has been extended to semiconductor alloy[38] systems in the zinc-blende structure using parameters of Harrison.[52] Estimates of the local environment effects on impurity levels have been carried out using the above perturbational approach and with the Harrison parameters for the $GaAs_xSb_{1-x}$ alloy system, to be reported on shortly, and the level splitting due to the local environment for the case of $x=0.5$ is found to be of the order of 30 to 40 meV for an impurity on the Ga site (four neighbors), and 5–20 meV for the case of an impurity on the As-Sb site (12 second neighbors). This figure falls in the range of experimental findings for these effects.[31] Finally, the more-sophisticated EMA calculations still need to be carried out. Further extensions to include off-diagonal disorder for an impurity need to be carried out in order to consider effects such as the bimodal distribution of nearest-neighbor bond lengths.[53]

ACKNOWLEDGMENTS

We would like to thank Vijay A. Singh for helpful conversations.

[1]P. Soven, Phys. Rev. **156**, 809 (1967).
[2]B. Velicky, S. Kirkpatrick, and H. Ehrenreich, Phys. Rev. B **175**, 847 (1968).
[3]D. W. Taylor, Phys. Rev. B **156**, 1017 (1967).
[4]R. J. Elliot, J. A. Krumhansl, and P. L. Leath, Rev. Mod. Phys. **46**, 465 (1974).
[5]E. Muller-Hartman, Solid State Commun. **12**, 1269 (1973).
[6]R. Mills and P. Ratanavararaksa, Phys. Rev. B **18**, 5291 (1978).
[7]F. Ducastelle, J. Phys. C **7**, 1795 (1974).
[8]B. G. Nickel and J. A. Krumhansl, Phys. Rev. B **4**, 4354 (1971).
[9]R. Alben, M. Blume, H. Krakauer, and L. Shwartz, Phys. Rev. B **12**, 4090 (1975).
[10]H. Shiba, Prog. Theor. Phys. **46**, 77 (1971).
[11]F. Browers, M. Cyrot, and F. Cyrot-Lackmann, Phys. Rev. B **7**, 4370 (1973); see also, F. Browers, F. Ducastelle, F. Cautier, and J. Van Der Rest, J. Phys. F **3**, 2120 (1973); F. Browers and F. Ducastelle, *ibid.* **5**, 45 (1975).
[12]J. A. Blackman, D. M. Esterling, and N. F. Berk, Phys. Rev. B **4**, 2412 (1971); J. A. Blackman, J. Phys. F **3**, L31 (1973).
[13]H. Fukuyama, H. Krakauer, and L. Schwartz, Phys. Rev. B

10, 1173 (1974).
[14]E-Ni Foo, H. Amar, and M. Auslos, Phys. Rev. B **4**, 3350 (1971).
[15]T. Kaplan, P. L. Leath, L. J. Gray, and H. W. Diehl, Phys. Rev. B **21**, 4230 (1980). See also, T. Kaplan and L. J. Gray, *ibid.* **29**, 3684 (1984) for references.
[16]M. Tsukada, J. Phys. Soc. Jpn. **26**, 684 (1969); **32**, 1475 (1972).
[17]W. H. Butler, Phys. Rev. B **8**, 4499 (1973).
[18]A. Mookerjee, J. Phys. C **6**, 1340 (1973), **6**, L205 (1973).
[19]A. R. Bishop and A. Mookerjee, J. Phys. C **7**, 2165 (1974). See A. Mookerjee, *ibid.* **8**, 29 (1975); A. Mookerjee, V. K. Srivastava, and V. Choudry, *ibid.* **16**, 4555 (1983) for extensions.
[20]R. L. Jacobs, J. Phys. F **3**, 933 (1973).
[21]A. K. Sen, R. Mills, T. Kaplan, and L. J. Gray, Phys. Rev. **30**, 5686 (1984).
[22]H. Miwa, Prog. Theor. Phys. **52**, 1 (1974).
[23]K. Aoi, Solid State Commun. **14**, 929 (1974).
[24]A. Gonis and J. W. Garland, Phys. Rev. B **31**, 2424 (1977).
[25]A. Zin and E. Stern, Phys. Rev. B **31**, 4954 (1985).
[26]P. L. Leath, *Excitations in Disordered Systems,* edited by M. F. Thorpe (Plenum, New York, 1981), p. 109.
[27]B. G. Nickel and W. H. Butler, Phys. Rev. Lett. **30**, 373 (1973).
[28]K. C. Hass, R. J. Lempert, and H. Ehrenreich, Phys. Rev. Lett. **52**, 77 (1984).
[29]H. Diehl and P. Leath, Phys. Rev. B **19**, 587 (1979); **19**, 596 (1979); and **19**, 5044 (1979).
[30]R. Haydock, V. Heine, and M. Kelly, J. Phys. C **5**, 2845 (1972).
[31]L. Samuelson, S. Nilson, Z.-G. Wang, and H. G. Grimmeiss, Phys. Rev. Lett. **53**, 1501 (1984), **54**, 850 (1985); *Proceedings of the International Conference on Defects in Semiconductors* (AIME, Warrendale, PA, 1987), p. 101. See also, H. Mariette, J. Chevallier, and P. Leroux-Hugon, Phys. Rev. B **21**, 5706 (1980); P. A. Murawala, V. A. Singh, S. Subramanian, S. S. Chandvankar, and B. M. Aurora, *ibid.* **29**, 4807 (1984).
[32]C. W. Myles and J. D. Dow, Phys. Rev. B **19**, 4939 (1979); **25**, 3593 (1982); Yu-Tang Shen and C. W. Myles, *ibid.* **30**, 3283 (1984); A. W. Gonis, W. H. Butler, and G. M. Stocks, Phys. Rev. Lett. **50**, 1482 (1983); A. Gonis and A. J. Freeman, Phys. Rev. B **31**, 2506 (1985).
[33]W. C. Ford and C. W. Myles, Phys. Rev. B **34**, 927 (1986); W. C. Ford, C. W. Myles, and Y.-T. Shen, *ibid.* **32**, 3416 (1985); C. W. Myles and W. C. Ford, J. Vac. Sci. Technol. A **4**, 2195 (1986).
[34]A. M. Mbaye and H. Mariette, J. Phys. C **17**, 6663 (1984).
[35]L. M. Roth, Phys. Rev. B **9**, 2476 (1974).
[36]L. M. Roth, Phys. Rev. B **11**, 3769 (1975).
[37]L. M. Roth, J. Phys. C **12**, 4879 (1979), J. Appl. Phys. **49**, 2139 (1978).
[38]J. E. Hasbun, Ph.D. thesis, State University of New York at Albany, 1987.
[39]G. F. Koster and J. C. Slater, Phys. Rev. **95**, 1167 (1954).
[40]E. N. Economou, *Green's Functions in Quantum Physics,* 2nd ed. (Springer-Verlag, New York, 1983).
[41]M. Lax, Phys. Rev. **85**, 621 (1952).
[42]L. Nordheim, Ann. Phys. (Leipzig) **9**, 609 (1931); **9**, 641 (1931).
[43]H. Ehrenreich and L. M. Schwartz, *Solid State Physics,* edited by F. Seitz, D. Turnbull, and H. Ehrenreich (Academic, New York, 1976), Vol. 31, p. 149.
[44]H. P. Hjalmarson, P. Vogl, D. J. Wolford, and J. D. Dow, Phys. Rev. Lett. **44**, 810 (1980).
[45]H. Mariette, Solid State Commun. **38**, 1193 (1981).
[46]S. T. Pantelides, Rev. Mod. Phys. **50**, 797 (1978).
[47]J. R. Jelitto, J. Phys. Chem. Solids **30**, 609 (1969).
[48]L. Shwartz and H. Ehrenreich, Phys. Rev. B **6**, 2923 (1972).
[49]W. E. Spicer, J. A. Silverman, J. Morgen, J. Lindau, J. A. Wilson, A.-B. Chen, and A. Sher, Phys. Rev. Lett. **49**, 948 (1982).
[50]A.-B. Chen and A. Sher, J. Vac. Sci. Technol. **21**, 138 (1982).
[51]K. C. Hass, H. Ehrenreich, and B. Velicky, Phys. Rev. B **27**, 1088 (1983).
[52]W. A. Harrison, *Electronic Structure and the Properties of Solids* (Freeman, San Francisco, 1980).
[53]J. C. Mikkelsen, Jr. and J. B. Boyce, Phys. Rev. Lett. **49**, 1412 (1982); A. Balzarotti, N. Motta, A. Kisiel, M. Zimmal-Starnawska, M. J. Czyzyk, and M. Podgorny, Phys. Rev. B **31**, 7526 (1980).